ResearchGate

See discussions, stats, and author profiles for this publication at: https://www.researchgate.net/publication/365750902

A new numerical limit analysis-based strategy to retrofit masonry curved structures with FRCM systems

Conference Paper · January 2022

DOI: 10.23967/eccomas.2022.020

CITATIONS
0

READS
14

5 authors, including:

Rebecca Fugger
Università Degli Studi Roma Tre
12 PUBLICATIONS **14** CITATIONS
SEE PROFILE

Ricardo Maia Avelino
ETH Zurich
14 PUBLICATIONS **57** CITATIONS
SEE PROFILE

Antonino Iannuzzo
Swinburne University of Technology
50 PUBLICATIONS **558** CITATIONS
SEE PROFILE

Gianmarco de Felice
Università Degli Studi Roma Tre
172 PUBLICATIONS **4,734** CITATIONS
SEE PROFILE

Some of the authors of this publication are also working on these related projects:

Masonry and stone arch bridges View project

Masonry View project

All content following this page was uploaded by Rebecca Fugger on 01 December 2022.

The user has requested enhancement of the downloaded file.

The 8th European Congress on Computational Methods in Applied Sciences and Engineering
ECCOMAS Congress 2022
5 – 9 June 2022, Oslo, Norway

A NEW NUMERICAL LIMIT ANALYSIS-BASED STRATEGY TO RETROFIT MASONRY CURVED STRUCTURES WITH FRCM SYSTEMS

R. FUGGER[1]*, R. MAIA AVELINO[2]†, A. IANNUZZO[3]†, P. BLOCK[4]† AND G. DE FELICE[5]*

*Roma Tre University, Department of Engineering,
Via Vito Volterra 62,
00146 Rome, Italy,
[1]rebecca.fugger@uniroma3.it, [5]gianmarco.defelice@uniroma3.it
https://www.romatrestrutture.eu/

† ETH Zurich, Institute of Technology in Architecture,
Block Research Group Stefano-Franscini-Platz 1, HIB E 45,
8093 Zürich, Switzerland,
[2]maia@arch.ethz.ch, [3]iannuzzo@arch.ethz.ch, [4]block@arch.ethz.ch
https://www.block.arch.ethz.ch/

Key words: Retrofitting, FRCM, Thrust Network Analysis, curved structures, arches, cross-vault.

Abstract. In most historic masonry structures, curved geometries, such as arches or vaults, are key structural components to the overall building stability. Therefore, it is crucial to assess their safety level with respect to changes in the boundary conditions (increased loads or settlements). If the safety level of the structure needs to be enhanced, a strategy to intervene and retrofit structural members is represented by the use of Fabric Reinforced Cementitious Matrix (FRCM) systems. These types of externally bonded composite materials, made of high-strength textiles embedded in inorganic matrices, are proven to be a particularly advantageous strengthening solution for curved masonry structures. Even though limit analysis approaches such as Thrust Network Analysis (TNA) have been widely used to assess structural stability, their use in a retrofitting framework is seldom explored. This paper proposes an automated procedure to design the FRCM reinforcement required in masonry structures based on an initial TNA assessment analysis. To perform these analyses, a nonlinear programming problem is implemented and solved to compute the minimum reinforcement required for stability. These quantities are then used to design the FRCM reinforcement according to existing regulations. Finally, the load-bearing capacity of the reinforced structure can be re-evaluated for different load cases ensuring that the structure is safe. The effectiveness of the proposed approach is benchmarked against laboratory tests and demonstrated on arched structures.

1 INTRODUCTION

Repair, or retrofit, existing masonry structures is sometimes required to restore the strength of damaged structural elements or to upgrade their original strength following a repurposing, with different load conditions etc. Nowadays, several techniques have been proposed as retrofitting solutions such as externally bonded reinforcements made of high strength textiles embedded in inorganic matrices. For this type of strategy, the textile adopted can range from natural materials such as basalt or glass to steel wires. They are better known as Fabric Reinforced Cementitious Matrix composite systems (FRCM) and have been studied as a reinforcing strategy for masonry structures in [1, 2, 3].

Indeed, several experimental campaigns have been carried out to determine the mechanical properties of FRCM systems applied with and without substrate [4, 5, 6, 7]. These systems proved to be a promising and effective solution in the construction field, designed by following existing regulations [8] and also approaches available in the literature [9, 10]. Nevertheless, the integration and design of FRCM systems for 3D structures is still an open topic, which needs to be explored.

As for the assessment of existing masonry structures, Heyman [11] shows that Limit Analysis can be applied given that three key assumptions are considered: no tensile strength, infinite compressive strength and no sliding. Nowadays, 3D approaches based on the lower-bound theorem of limit analysis have been developed, such as Thrust Network Analysis [12, 13] which uses a compressive network, or the Thrust Membrane Analysis [14] as well as the ones presented in [15, 16, 17, 18, 19, 20].

In this framework, the present paper provides with a strategy to retrofit masonry 2D curved structures adopting FRCM systems. To compute the minimum amount of reinforcement needed, an optimisation procedure of thrust network analysis is implemented. The optimisation procedure allows the thrust network to go outside the thickness, both at the intrados and extrados, by adding a virtual additional thickness as a variable of the problem as in [21]. In this way, the output of the optimisation can be used to compute the amount of FRCM needed. The hypothesis of simultaneous rupture of the FRCM and masonry in a cross-section analysis is the starting point for the design of the quantity of reinforcement needed.

To validate this strategy, two case studies have been considered. First, the circular arch tested in [22, 23] reinforced with a PBO-FRCM either only in the intrados or in the extrados surface. Second, the barrel vault with buttresses and filling tested in [24] is revisited, strengthened with a basalt-FRCM.

2 THRUST NETWORK OPTIMISATION

2.1 Thrust Network Analysis equilibrium

Thrust Network Analysis (TNA) [12, 25] is an equilibrium method that allows for finding admissible stress solutions in masonry vaulted structures. With TNA, the internal stresses of masonry structures are modelled as a connected network, with axial forces in the edges and loads applied to its nodes. We assume a network with m edges and n vertices, being n_i free and n_b fixed vertices. The statical variable controlling the forces in the network is the edge's force density, stored in the vector $\mathbf{q}$ [m x 1]. After [26], the force density of an edge is defined as the ratio among the axial force in the edge and its length.

Following the formulation of [13, 27], the horizontal projection of the networks studied in this work is assumed to be fixed and is named *form diagram*. This reduces the indeterminacy of the problem, consequently reducing the number of free variables describing the internal equilibrium of the network. As such, only the force densities of the *k* independent edges are taken as variables and a vector of force densities is retrieved through the linear mapping:

$$\boldsymbol{q} = \boldsymbol{B}\boldsymbol{q}_{id} + \boldsymbol{d}, \text{ with: } \boldsymbol{B} = \begin{bmatrix} \frac{-\boldsymbol{E}_d^{\dagger}\boldsymbol{E}_{id}}{\boldsymbol{I}_k} \end{bmatrix}, \boldsymbol{d} = \begin{bmatrix} \frac{\boldsymbol{E}_d^{\dagger}\boldsymbol{p}_{h,i}}{\boldsymbol{0}} \end{bmatrix}, \tag{1}$$

in which, $\mathbf{E}$ [$2n_i$ x m] is the horizontal equilibrium matrix (see [13]), $\mathbf{p}_{h,i}$ [$2n_i$ x *1*] is the vector storing horizontal forces applied to the internal nodes, $\mathbf{I}_k$ [k x k] is the identity matrix of size k, and the subscript "d" and "id" corresponds to the slicing in the dependent and independent edges, respectively.

Following this formulation, the free elevations of the network are computed in terms of the independent force densities $\mathbf{q}_{id}$ and the height of the supports $\mathbf{z}_b$

$$\boldsymbol{z}_i(\boldsymbol{q}_{id}, \boldsymbol{z}_b) = (\boldsymbol{C}_i^T \boldsymbol{Q} \boldsymbol{C}_i)^{-1}\left(\boldsymbol{p}_{z,i} - (\boldsymbol{C}_i^T \boldsymbol{Q} \boldsymbol{C}_b)\boldsymbol{z}_b\right) \tag{2}$$

in which $\mathbf{p}_{z,i}$ [n_i x *1*] is the vector storing vertical forces applied to free nodes, $\mathbf{C}$ is the well-known connectivity matrix [26] and $\mathbf{Q}$ = diag($\mathbf{q}$).

2.2 Admissible Thrust Networks for Masonry Structures

From the infinite spatial networks with fixed form diagram arising from the methodology described, only the ones respecting Heyman's limit analysis criterion are considered admissible to masonry structures. From Heyman's assumptions, limit analysis can be applied to masonry structures given that (i) compression strength is assumed infinite, (ii) tensile strength is null and (iii) no sliding occurs. As highlighted in [13], these assumptions translate into compressive forces in the thrust networks (Eq. 3.1) and in enforcing the heights of the network within the envelope of the masonry described through elevations z^{LB}_i for the intrados and z^{UB}_i for the extrados (Eq. 3.2).

$$q_i \leq 0 \qquad \text{for} \quad i = [1, 2, \dots, m], \tag{3.1}$$

$$z_i^{LB} \leq z_i \leq z_i^{UB} \qquad \text{for} \quad i = [1, 2, \dots, n], \tag{3.2}$$

In [4], this criterion is coupled to optimisation algorithms to find admissible stress states minimising and maximising horizontal thrust and also maximising the geometric safety factor (GSF). In [27], this framework is applied to compute the GSF of parametric groin vaults.

2.3 Increasing capacity considering virtual thicknesses

When the optimisation search described in Section 3.2 does not find any solution (i.e., the problem is infeasible), the structure analysed cannot be considered safe from a lower-bound limit analysis standpoint. This might occur, e.g., when the thickness of the structure is insufficient, or an extreme external load is imposed. In this paper, we focus on the latter, and we introduce a strategy to increase the space of admissibility of the problem by virtually increasing the structural thickness, as in [21]. This additional thickness is provided by the addition of FRCM reinforcement in critical locations and following a specific layout.

Numerically, this reflects in a new nonlinear optimisation problem (NLP) solved by introducing 2n variables representing virtual additional thicknesses t^{UB}_i and t^{LB}_i effectively increasing the allowable thickness to node i of the network in the extrados and intrados

respectively. The objective of the optimisation is then the minimisation of the additional virtual thickness (in the least square sense). The complete optimisation problem is presented below.

$$\underset{\boldsymbol{q}_{ind},\boldsymbol{z}_b,\boldsymbol{t}^{UB},\boldsymbol{t}^{LB}}{\text{minimise}} \quad \sum_i^n (t_i^{UB})^2 + (t_i^{LB})^2 \tag{4.1}$$

$$\textit{subject to} \quad q_i \leq 0 \qquad \text{for} \quad i = [1, 2, \dots, m], \tag{4.2}$$

$$z_i^{LB} - t_i^{LB} \leq z_i \leq z_i^{UB} + t_i^{UB} \qquad \text{for} \quad i = [1, 2, \dots, n], \tag{4.3}$$

$$t_i^{UB} \geq 0, \qquad \text{for} \quad i = [1, 2, \dots, n] \tag{4.4}$$

$$t_i^{LB} \geq 0, \qquad \text{for} \quad i = [1, 2, \dots, n] \tag{4.5}$$

The optimisation problem presented in Eq. 4 is solved with interior point methods [28]. The starting point is the well-known load-path optimisation, as in [21]. Gradient and Jacobian matrices are provided analytically to the solving engine. The implementation is carried through the python package *compas_tno* [29] developed to perform assessment of vaulted masonry structures.

Having computed the minimum additional thickness required and the distribution of this additional thickness in the footprint of the masonry vaulted structure, the amount of reinforcement can be calculated as described in Section 4.

3 DESIGN OF THE REINFORCEMENT

3.1 Cross-section analysis

The first estimation of FRCM reinforcement needed is provided using a limit analysis approach [8]. It is assumed that both FRCM, in tension, and masonry, in compression attain their maximum stress, neglecting any strain compatibility, as represented in Fig 1. Hence, the resultant internal forces F_f and F_m exerted by the reinforcement and the masonry respectively can be evaluated as follows:

$$F_f = f_{fd} A_f, \tag{5.1}$$

$$F_m = \xi f_m \beta c_u B. \tag{5.2}$$

Where:

- A_f is the area of reinforcement needed,
- f_{fd} is the design tensile stress of the FRCM considered;
- the product between ξ and f_m is the compressive strength of masonry over a depth $\beta\, c_u$;
- B is the width of the cross-section.

The neutral axis depth is provided by the equilibrium equation for the current axial load N, according to Eq. 6:

$$F_f + N = F_m \tag{6}$$

By solving Eq. 7, which equals the resistant moment of the reinforced cross-section and the bending moment M, the minimum amount of reinforcement needed is given by Eq. (8):

$$F_f \frac{t}{2} + F_m \left(\frac{t}{2} - \frac{c_u}{2}\right) = M, \tag{7}$$

$$A_{fmin} = \frac{1}{f_{fd}}\left(\psi - N + \sqrt{\psi^2 - \psi N - \frac{2M\psi}{t}}\right) \quad (8)$$

Where $\psi = Bt\xi f_m$ and t is the thickness of the cross-section.

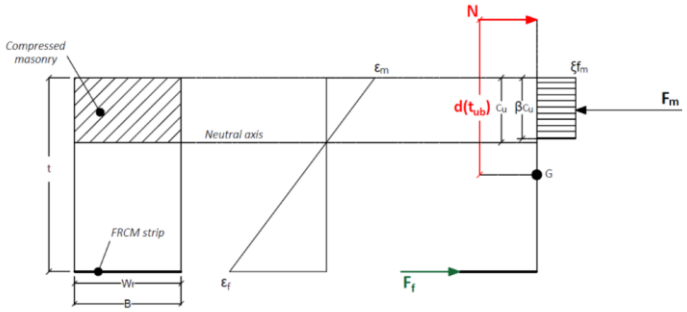

Figure 1: Cross-section assumed showing the compressed masonry and the FRCM reinforcement applied. The strain and stress profile and the internal forces in the cross-section are highlighted.

3.2 Cross-section identification

In 2D structures such as arches, it is straightforward to consider the nodes of the thrust as joints of the masonry composing the structure. Therefore, as represented in Fig. 2, the cross-sections can be identified as perpendicular to the middle line of the masonry. More specifically, they are placed in the intersection between the middle line and the vertical line associated with each node of the thrust line. Hence, the directions either perpendicular (η) or parallel (ξ) to the cross-section are defined (see $\eta x \xi$ coordinate system in Fig. 2) and so the forces and bending moments can be evaluated in order to calculate the minimum amount of reinforcement needed as described in Section 3.1.

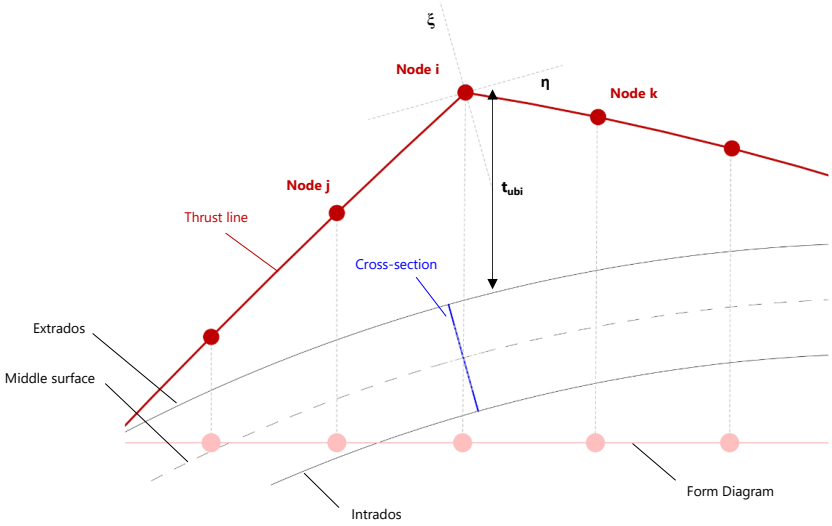

Figure 2: Longitudinal view of a thrust line (red) outside of the extrados of the curved masonry structure showing the cross-section identification (blue) and highlighting the additional virtual thickness ($t_{ub,i}$) at node i.

Each node is subjected to its self-weight and the thrusts of the edges arriving at the node (p_{zi}, f_{ji}, f_{ik} shown in Fig. 3a. In order to evaluate the normal force acting into the cross-section, the thrusts of the two edges converging into the node (f_{ji}, f_{ik}) are projected in the $\eta x \xi$ system, hence N_{ji} and N_{ik} are defined. They have different intensities, since there is a discontinuity due to the fact that the equilibrium is not being made along the horizontal direction. To overcome this problem, the norm force which will provide the higher amount of minimum reinforcement is considered for the reinforcement calculation.

On the other hand, the bending moment is simply evaluated as the product between the horizontal force acting into the node and the distance of the node from the middle surface. The horizontal force f_{hi} is again evaluated by the horizontal projection of the thrusts f_{ji}, f_{ik}. While the distance considered in the calculation of the bending moment is the sum between the virtual additional thickness needed in that node t_{ubi} and half of the thickness of the structure (t/2), see Fig. 3c. The aforementioned evaluation of the bending moment results to be more consistent within the general TNA approach where all the horizontal forces are in equilibrium and, also, uses directly the output of the optimisation procedure described in Section 2.

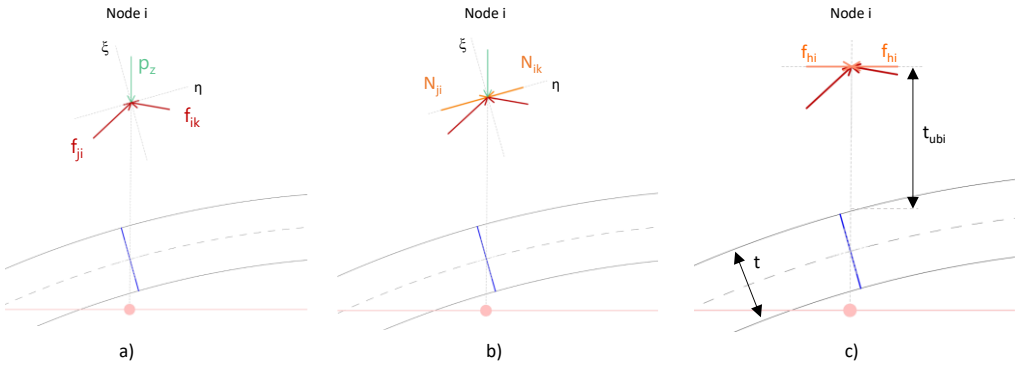

Figure 3: a) forces acting into node i; b) projection of the thrusts to identify the norm force acting in the cross-section; c) horizontal force in the node and distances to be considered in the evaluation of the bending moment.

4 APPLICATIONS

In order to apply the presented strategy, two case studies are studied, first a simple arch tested in [22, 23] and second, a buttressed arch tested in [24].

4.1 Simple arch

The geometry of the arch tested in [22, 23] is schematically represented in Fig. 4. It has a span of 1500 mm, an intrados radius of 866 mm, a rise of 432.5 mm, a thickness and an out-of-plane width of 95 mm. Three types of tests were performed: unreinforced arch, reinforced arch with PBO-FRCM composite either applied in the whole intrados and extrados. Each arch was loaded at a distance of 375 mm from the left abutment and the reached average peak load was 1.0 kN when unreinforced, 5.4 kN when reinforced at the intrados and 4.9 kN when reinforced at the extrados. As for the reinforcement used, a bi-directional PBO textile (11x11 mm^2 grid-spacing) is embedded in a cement-based mortar. The design thickness is 0.014 mm and the tensile strength is 5700 MPa, hence the area of FRCM applied is 1.33 mm^2 distributed over the out-of-plan width.

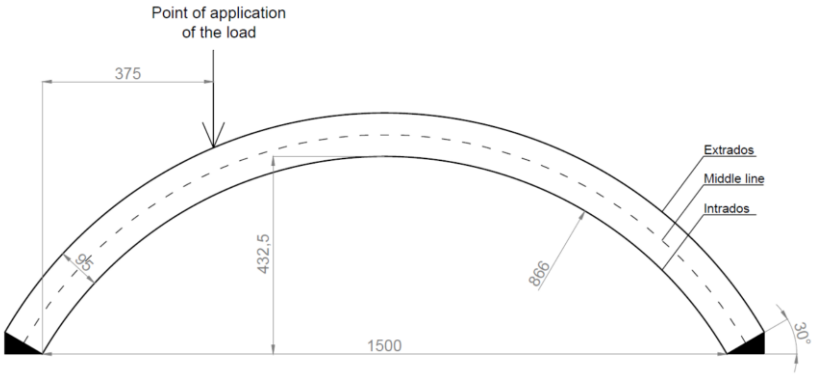

Figure 4: Geometry of the arch tests in [22, 23] highlighting the point of application of the load.

Fig. 5 shows the amount of reinforcement needed in each cross-section, A_{num}, which correspond to each node of the form diagram as explained in Section 4.2, and the amount of reinforcement applied during the experiment A_{exp}. More specifically, Fig. 5a represents the arch loaded with 5.4 kN allowing the thrust network to go outside of the extrados, hence, only t_{ub} is a parameter of the optimisation procedure. On the other hand, in Fig. 5b the arch is loaded with 4.9 kN and the thrust can go only outside of the intrados, meaning that only t_{lb} is allowed. It can be appreciated from both cases that the minimum amount of reinforcement obtained applying the presented procedure well approximates the real amount of reinforcement. Especially, when only t_{ub} is allowed, the loaded node and the corresponding cross-section returns the same area of FRCM applied in the experiments (-1% of difference), while in the second case the difference in the most critical cross-section is about -22%.

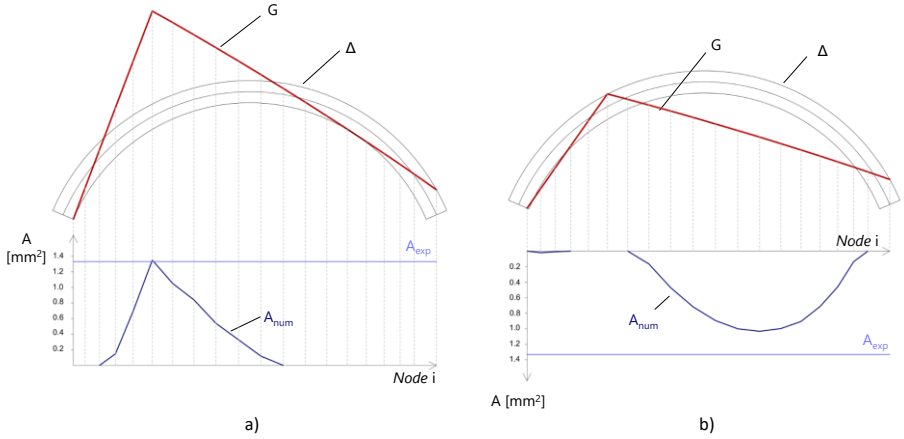

Figure 5: Minimum amount of reinforcement needed when the average peak load reached when a) the FRCM is applied at the intrados, 5.4kN; b) the FRCM is applied at the intrados, 4.9kN.

4.2 Buttressed arch

The frontal view of the barrel vault with buttresses and filling, tested in [24], is schematically represented in Fig. 6a. The arch has a span of 2790 mm, a height of 650 mm and a thickness of 55 mm. The out-of-plane width is 500 mm for the arch and 120 mm for the buttresses. As well as for the simple arch case study, three types of tests were carried out: unreinforced arch, reinforced arch with basalt-FRCM composite either applied either in the intrados and extrados

surface. The additional load is applied at a distance of 906 mm from the right abutment. This experimental campaign provides either the load when hinges are activated, P_H, or the peak load reached during the tests, P_L. The load activating the hinges is around P_H=4.0 kN, P_H^{LB}=5.6 kN and P_H^{UB}=8.0 kN when the arch is unreinforced, reinforced at the intrados and reinforced at the extrados respectively. While, the peak load is equal to P_L=5.9 kN, P_L^{LB}=10.1 kN and P_L^{UB}=14.1 kN respectively in the same three cases as above. The FRCM used is a bi-directional basalt textile with 9x9mm^2 grid-spacing embedded in a lime-based mortar. The design thickness is 0.064 mm and the ultimate strength is 390 MPa, hence the area of FRCM applied is 32 mm^2 in the entire width of the arch.

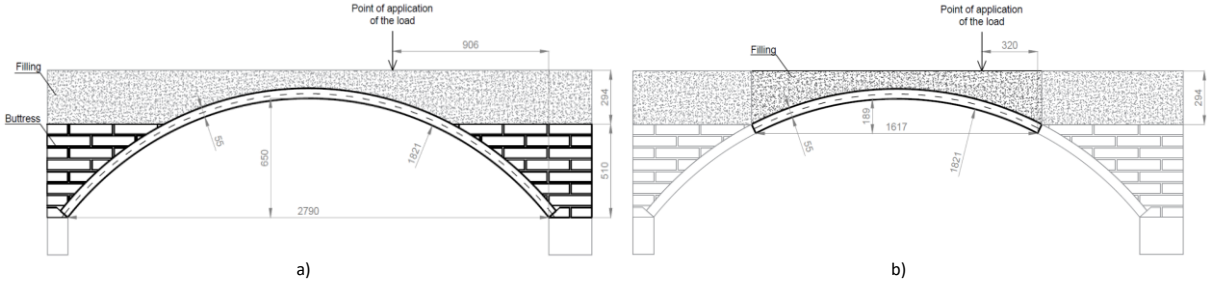

Figure 6: a) Frontal view of the barrel vault with buttresses tested in [24], as well as the first geometry considered in the analyses; b) second geometry considered in the analyses.

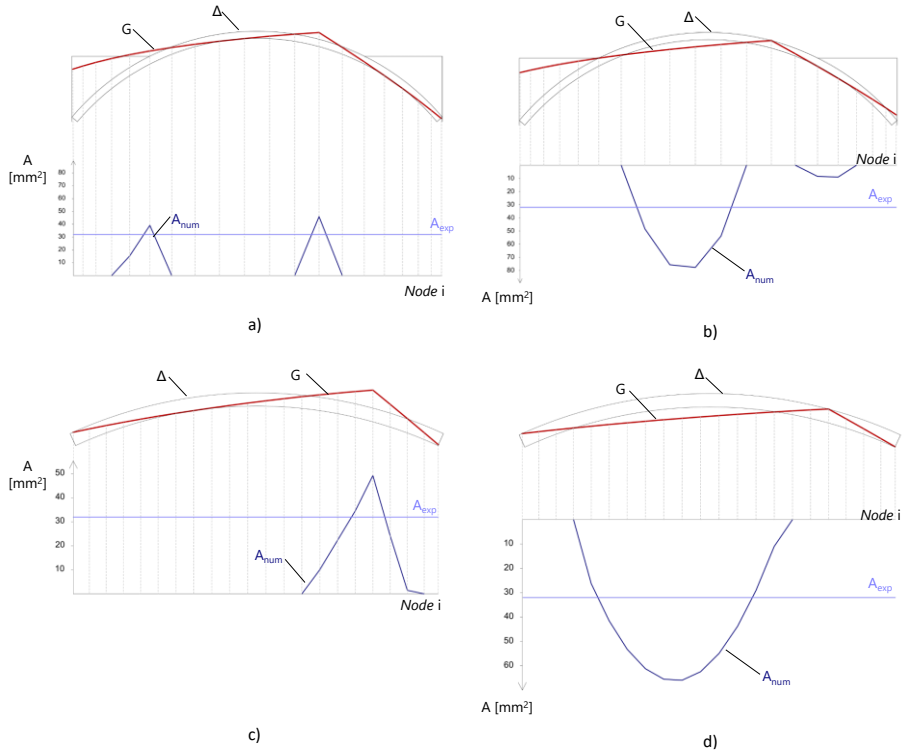

Figure 7: Minimum amount of reinforcement needed when P_L is applied, considering the first geometry a) and b), and considering the second geometry c) and d). FRCM applied at the intrados and loaded with P_L^{LB} = 10.1kN a) and c). FRCM applied at the extrados and loaded with P_L^{UB} = 14.1kN b) and d).

Since this case study presents a more complex structure, two different geometries have been considered in the application of the presented strategy. The first one considers the entire arch modeled together with the buttresses as structural elements (Fig. 6a), meaning that the thrust can move into them. While, the second one is the shallow arch in between the two buttresses and is depicted in Fig. 6b. In both cases, the filling is also considered with a specific weight of 12.5 kN/m^3, and added ad a weight to each node of the form diagram.

Fig. 7a and b show the results of the applied strategy when the first geometry is considered and the values of P_L are applied. Fig. 7c and d show the results when the same loads are applied to the second geometry. It can be noted that in all cases, A_{num} obtained presents deviations from the amount of FRCM used in the experiments. It has been observed that the amounts calculated are higher than the quantities applied. A reason for such over-conservatism can be the fact that the structure, when the peak load is reached, presents a 3D behaviour that cannot be neglected by modelling it as a 2D arch. Moreover, the external loads in the models are applied to a sole node, a while distribution among neighbour nodes would also be considered.

Following, the load which corresponds to the creation of the hinges has been applied to the same two geometries and the results are shown in Fig. 8. As expected, in these analyses, A_{num} is reduced, as the loads are smaller, and they fall under the real amount of reinforcement applied in three of the four cases. The differences considering the first geometry are around -28% and +21%, allowing t_{ub} and t_{lb} respectively. While, if the single arch is considered A_{num} differs from A_{exp} by -31% and +1%.

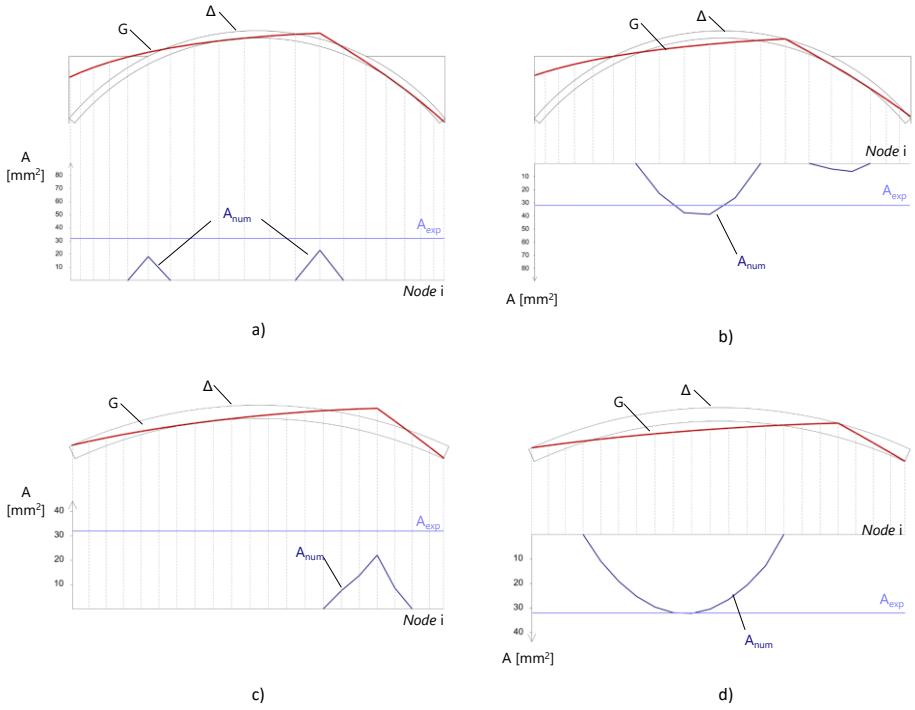

Figure 8: Minimum amount of reinforcement needed when P_H is applied, considering the first geometry a) and b), and considering the second geometry c) and d). FRCM applied at the intrados and loaded with P_H^{LB} = 5.6kN a) and c). FRCM applied at the extrados and loaded with P_H^{UB} = 8.0kN b) and d).

5 CONCLUSIONS

This paper provides a strategy to design an externally bonded reinforcement (FRCM) retrofitting intervention on curved structures having quantities based on a thrust network analysis. An optimization procedure is presented in order to virtually increase the structural thickness when the structure cannot be considered safe from a lower-bound limit analysis point of view. In this way, the output of the given optimisation can be directly used in the design of FRCM systems either in 2D structures, such as arches, or in 3D structures, such as cross-vaults. Hence, the design of the FRCM is carried out through a cross-section analysis, following existing regulations. The key point is, therefore, to identify a cross-section in a general configuration. This is done by considering a cross-section to each node of the form-diagram used in the thrust network

The proposed strategy has been applied to two different case studies: a simple arch and a buttressed arch. The first case study revisits an experimental campaign conducted in a similar geometry and the results of FRCM quantities are close to the ones applied in the tests (no error when reinforced at the intrados and error of 20% when at the extrados). The second case study also corresponds to an experimental campaign, however the buttressed arch of this example presented a more complex geometry which resulted in less accurate approximations when the peak load reached in the experiments is applied, since 3D behaviour may have to be considered.

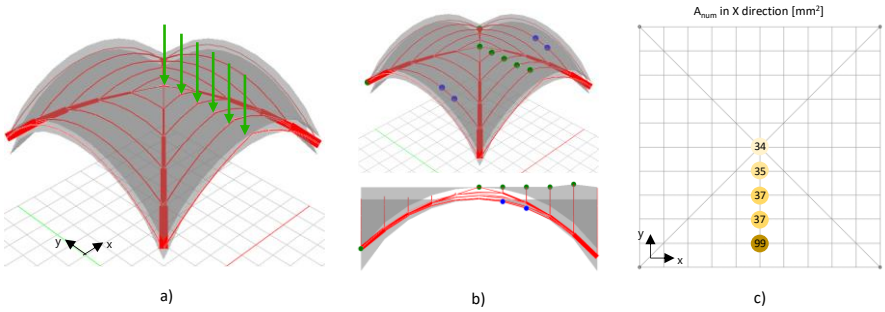

Figure 9: a) 3D geometry of a shallow cross-vault with additional line load, b) thrust network leaving the structural section; b) minimum amount of reinforcement computed by the proposed methodology in x-direction.

The present methodology could be also extended to 3D structures, since a tool to design an externally bonded reinforcement for those types of structures is, nowadays, not yet available. Therefore, the three-dimensional extension will be the core of a future contribution by the authors. Indeed, Figure 9a shows a shallow cross vault (10x10 m^2 in plan and a thickness of 0.5 m) in which an additional line load of 26 kN/m (2% of the total self-weight) is applied in the centre of one web. Figure 9b shows the thrust network exiting the structural geometry, allowing only t_{UB} and Figure 9c shows the quantities of FRCM reinforcement calculated for the reinforcement applied in x-direction. This calculation is possible by considering the forces decomposed in the directions of the FRCM strips are fixed a priori (x and y in this case). The cross section is defined for each node of the form diagram and is oriented perpendicular to the direction of the reinforcing strip following the direction of the normal with respect to the middle surface in the node observed.

The merit of the numerical formulation applied is the simplicity of the input and the comprehensive output, which allows it to be easily interpreted by engineers working in assessment and retrofitting of masonry structures.

Finally, the results obtained were, in most of the cases, overly conservative. Future work will be focused in reducing this conservatism and obtaining more accurate measurement. For three-dimensional structures, for example, different form diagrams should be explored in order to obtain a lower minimum reinforcement area. Furthermore, the analysis of different load cases can be applied, in order to define which is the most severe configuration in terms of quantity of reinforcement to be added.

REFERENCES

[1] Papanicolaou, C., Triantafillou, T., Karlos, K. and Papathanasiou, M. Textile reinforced mortar (TRM) versus FRP as strengthening material of URM walls: In-plane cyclic loading. *Mat. and Str.*, (2007) **40**:1081-1097.

[2] Papanicolaou, C., Triantafillou, T., Papathanasiou, M and Karlos, K. Textile reinforced mortar (TRM) versus FRP as strengthening material of URM walls: out- of- plane cyclic loading. *Mat. and Str.*, (2008) **41**:143-157.

[3] de Felice G., D'Antino T., De Santis S., Meriggi P. and Roscini, F. Lessons Learned on the Tensile and Bond Behavior of Fabric Reinforced Cementitious Matrix (FRCM) Composites. *Frontiers in Built Environment.*, (2020) **6**.

[4] De Santis S., de Felice, G., Di Noia, G. L., Meriggi, P. and Volpe M. Shake table tests on a masonry structure retrofitted with composite reinforced mortar. *6th Int. Conf. on Mechanics of Masonry Str. Strengthened with Composite Materials* (2019).

[5] Fares S., Fugger R., De Santis S. and de Felice G. Tensile and Pull-Out Behavior of Steel Reinforced Grout Connectors. *Int. Workshop on Engineering Materials for Sustainable Structures* (2021).

[6] Fugger R., Fares S., Meriggi P., Nerilli F., Marfia S., Sacco E. and de Felice G. Testing of Fabric Reinforced Cementitious Matrix in Shear without Substrate. *7th Int. Conf. on Mechanics of Masonry Str. Strengthened with Composite Materials* (2021).

[7] Fares S., Fugger R., De Santis S. and de Felice G. Strength, bond and durability of stainless steel reinforced grout. *Constr. and Buil. Mat.*, (2022) **322:**126465.

[8] ACI. Guide to Design and Construction of Externally Bonded Fabric-Reinforced Cementitious Matrix (FRCM) and Steel-Reinforced Grout (SRG) Systems for Repair and Strengthening Masonry Structures. ACI 549.6 R-20. (2020). Farmington Hills, MI, US.

[9] Meriggi P., de Felice G. and De Santis S. Design of the out-of-plane strengthening of masonry walls with fabric reinforced cementitious matrix composites. *Constr. and Buil. Mat.*, (2020) **240**.

[10] Meriggi P., De Santis S., Fares S. and de Felice G. Design of the shear strengthening of masonry walls with fabric reinforced cementitious matrix. *Constr. and Buil. Mat.*, (2021) **279**.

[11] Heyman J. The Stone Skeleton. *Int. J. of sol. and str.*, (1966) **2:**249-279.

[12] Block P. and Ochesendorf J. Thrust Network Analysis: A New Methodology for 3D Equillibrium. *J. of the Int. Ass. for Shell and Spatial Structures*, (2007) **48**:1-7.

[13] Maia Avelino R., Iannuzzo A., Van Mele T. and Block P. Assessing the Safety of Vaulted Masonry Structures Using Thrust Network Analysis. *Comp. & Str.* (2021) **257**.

[14] Olivieri C., Fortunato A. and DeJong M. A new membrane equilibrium solution for masonry railway bridges: the case study of Marsh Lane Bridge. *Int. J. of Masonry Research and Innovation,* (2021) **6:**446-471.
[15] Olivieri, C., Angelillo, M., Gesualdo, A., Iannuzzo, A., and Fortunato, A. Parametric design of purely compressed shells, *Mechanics of Materials*, (2021) **103782**., p. 155,
[16] Cusano, C., Montanino, A., Olivieri, C., Paris, V., and Cennamo, C., Graphical and analytical quantitative comparison in the domes assessment: the case of San Francesco di Paola (2021), *Applied Sciences*, **11(8)**, 3622.
[17] Angelillo, M, Olivieri C., andDeJong, M. A new equilibrium solution for masonry spiral stairs, *Engineering structures* (2021), **238**, p. 112176.
[18] Montanino, A., Olivieri, C., Zuccaro, G., and Angelillo, M., From stress to shape: equilibrium of cloister and cross vaults (2021), *Applied Sciences*, 11**(9)**, 3846.
[19] Nodargi N.A. and P. Bisegna, Thrust line analysis revisited and applied to optimization of masonry arches. *International Journal of Mechanical Sciences* (2020), **179**, p. 105690.
[20] Nodargi N.A. and P. Bisegna, A new computational framework for the minimum thrust analysis of axisymmetric masonry domes. *Engineering Structures* (2021), **234**, p. 111962.
[21] López López D., Roca Fabregat P., Liew A., Méndez Echenagucia T., Van Mele T. and Block P. A three-dimensional approach to the Extended Limit Analysis of Reinforced Masonry. *Structures* (2022) **35:**1062-1077.
[22] Alecci, V., Focacci, F., Rovero, L., Stipo G. and De Stefano, M. Extrados strengthening of brick masonry arches with PBO–FRCM composites: Experimental and analytical investigations. *Composite Structures* (2016) **149**:184-196.
[23] Alecci, V., Focacci, F., Rovero, L., Stipo G. and De Stefano, M. Intrados strengthening of brick masonry arches with different FRCM composites: Experimental and analytical investigations. *Composite Structures* (2017) **176**:898-909.
[24] De Santis, S., de Felice, G. and Roscini, F. Retrofitting of Masonry Vaults by Basalt Textile-Reinforced Mortar Overlays. *Int. J. of Arch. Her.* (2019) **13**:1061-1077.
[25] Block, P. and Lorenz, L. Three-Dimensional Funicular Analysis of Masonry Vaults. *Mechanics Research Communications,* (2014) **56:**53-60.
[26] Schek H-J. The Force Density Method for Form Finding and Computation of General Networks. *Computer Methods in Applied Mechanics and Engineering.* (1974) **3:**115-134.
[27] Maia Avelino R., Iannuzzo A., Van Mele T. and Block P. Parametric Stability Analysis of Groin Vaults. *Applied Sciences* (2021) **11(8).**
[28] Wächter A. and Biegler, L.T. On the Implementation of an Interior-Point Filter Line-Search Algorithm for Large-Scale Nonlinear Programming. *Mathematical Programming.* (2006) **106**:25-57
[29] Maia Avelino R., COMPAS TNO: An implementation of constrained optimisation to thrust networks for the assessment of masonry structures, *https://blockresearchgroup.github.io/compas_tno*.

View publication stats